Physics Letters B 771 (2017) 487–491

Contents lists available at ScienceDirect

Physics Letters B

www.elsevier.com/locate/physletb

Testing χ_c properties at BELLE II ☆

Henryk Czyż *, Patrycja Kisza

Institute of Physics, University of Silesia, PL-40007 Katowice, Poland

ARTICLE INFO

Article history:
Received 23 December 2016
Received in revised form 31 May 2017
Accepted 31 May 2017
Available online 7 June 2017
Editor: B. Grinstein

Keywords:
χ_{c_i} properties
Monte Carlo generators

ABSTRACT

The model of the $\chi_{c_i} - \gamma^* - \gamma^*$ and $\chi_{c_i} - J/\psi^* - \gamma^*$ form factors developed in [1] for χ_{c_1} and χ_{c_2} is extended to χ_{c_0} case. The studies performed within this model have shown that at BELLE II it will be possible to study in detail $\chi_{c_i} - \gamma^* - \gamma$ form factors through measurements of the reaction $e^+e^- \to e^+e^-\chi_{c_i}(\to J/\psi(\to \mu^+\mu^-)\gamma)$. The results were obtained using the newly updated Monte Carlo generator EKHARA.

1. Introduction

Soon the BELLE II experiment [2] will start to operate with unprecedented luminosity allowing to access information not available before. In this letter we show that the integrated luminosity of 20–50 ab^{-1} will allow BELLE II collaboration to study in detail the $\chi_{c_i} - \gamma^* - \gamma$ form factors. These form factors are used in the calculations of the electronic widths of the χ_{c_i}, which were not yet measured. The theoretical predictions available for these widths [3–6,1] depend strongly on the details of the form factors modelling and are different, up to two orders of magnitude, even if all the models agree with experimental data [7] on the $\chi_{c_i} \to J/\psi\gamma$, $i = 1, 2$ and $\chi_{c_2} \to \gamma\gamma$ partial decay widths. We advocate here that the experimental studies of the reactions $e^+e^- \to e^+e^-\chi_{c_i}(\to J/\psi(\to \mu^+\mu^-)\gamma)$ can differentiate between the proposed models.

To give realistic predictions for event selections close to the experimental ones, we have extended the model developed in [1] to cover also $\chi_{c_0} - \gamma^* - \gamma^*$ amplitudes and implemented the model amplitudes in the event generator EKHARA [8,9]. The generator can also help in the data analysis of the reactions $e^+e^- \to e^+e^-\chi_{c_i}$ and $e^+e^- \to e^+e^-\chi_{c_i}(\to J/\psi(\to \mu^+\mu^-)\gamma)$. The newly updated code is available from the EKHARA web page (http://prac.us.edu.pl/~ekhara/).

The layout of this letter is the following: In Section 2 we describe the model used in the presented simulations. In Section 3 we give predictions for the expected number of events of the χ_{c_i} production cross sections at BELLE II and the expected number of events for the form factor measurements. The QED non-resonant background is discussed in Section 4. Conclusions are presented in Section 5.

2. The model

The model used in this letter is an extension of the model [1] built to describe χ_{c_1} and χ_{c_2} decays to $J/\psi\gamma$, the χ_{c_2} decay to $\gamma\gamma$ and ψ' decays to $\chi_{c_{1(2)}}\gamma$. The basic assumptions used to construct the amplitudes for χ_{c_0} decays to $J/\psi\gamma$ and $\gamma\gamma$ as well as ψ' decay to $\chi_{c_0}\gamma$ are the same as in [1]. We start from the $\chi_{c_i} - \gamma^* - \gamma^*$ amplitudes calculated in [3] and assume that the Lorentz structure, as well as the form factor, are identical also for $\chi_{c_i} - J/\psi^* - \gamma^*$ amplitude. We allow only for different coupling constants. From these assumptions one gets the following amplitudes for the decays $\chi_{c_0} \to \gamma\gamma$, $\chi_{c_0} \to J/\psi\gamma$ and $\psi' \to \chi_{c_0}\gamma$

$$
\begin{aligned}
A^{\alpha\beta}_{0\gamma\gamma}(p_1,p_2)\epsilon^1_\alpha\epsilon^2_\beta\Big|_{p_1^2=p_2^2=0} &= c^0_\gamma A(p_1,p_2),\\
A^{\alpha\beta}_{0\gamma J/\psi}(p_1,p_2)\epsilon^1_\alpha\epsilon^2_\beta\Big|_{p_1^2=0,\ p_2^2=M^2_{J/\psi}} &= c^0_{J/\psi} A(p_1,p_2),\\
A^{\alpha\beta}_{\psi'0\gamma}(p_1,p_2)\epsilon^1_\alpha\epsilon^2_\beta\Big|_{p_1^2=0,\ p_2^2=M^2_{\psi'}} &= c^0_{\psi'} A(p_1,p_2),
\end{aligned}
\tag{1}
$$

where $\epsilon^i \equiv \epsilon(p_i)$ are the appropriate polarisation vectors,

☆ Work supported in part by the Polish National Science Centre, grant number DEC-2012/07/B/ST2/03867.

* Corresponding author.
E-mail address: czyz@us.edu.pl (H. Czyż).

http://dx.doi.org/10.1016/j.physletb.2017.05.091

Table 1
Model parameters and theoretical (*th*) (this paper, see also [1]), and experimental (*exp*) [7] values of $\Gamma(\chi_{c_{0,1,2}} \to \gamma\gamma, \gamma J/\psi)$ and $\Gamma(\psi' \to \chi_{c_{0,1,2}}\gamma)$.

a [GeV$^{5/2}$]	m [GeV]	a_J [GeV$^{5/2}$]	a_J^0 [GeV$^{5/2}$]	$a_{\psi'}$ [GeV$^{5/2}$]	$a_{\psi'}^0$ [GeV$^{5/2}$]
0.0796	1.67	0.129	0.073	−0.078	0.122

Widths [MeV]	χ_{c_0}	χ_{c_1}	χ_{c_2}
$\Gamma(\chi \to \gamma\gamma)_{th}$	$2.24 \cdot 10^{-3}$	–	$5.46 \cdot 10^{-4}$
$\Gamma(\chi \to J/\psi\gamma)_{th}$	$1.34 \cdot 10^{-1}$	$2.82 \cdot 10^{-1}$	$3.74 \cdot 10^{-1}$
$\Gamma(\psi' \to \chi\gamma)_{th}$	$2.96 \cdot 10^{-2}$	$2.88 \cdot 10^{-2}$	$2.64 \cdot 10^{-2}$
$\Gamma(\chi \to \gamma\gamma)_{exp}$	$2.3(2) \cdot 10^{-3}$	–	$5.3(4) \cdot 10^{-4}$
$\Gamma(\chi \to J/\psi\gamma)_{exp}$	$1.3(1) \cdot 10^{-1}$	$2.8(2) \cdot 10^{-1}$	$3.7(3) \cdot 10^{-1}$
$\Gamma(\psi' \to \chi\gamma)_{exp}$	$2.96(11) \cdot 10^{-2}$	$2.8(1) \cdot 10^{-2}$	$2.7(1) \cdot 10^{-2}$

Table 2
Predictions of the electronic widths of the χ_{c_1} and χ_{c_2} charmonia within recently published models.

	[1]	[6]	[4]	[5]
$\Gamma(\chi_{c_1} \to e^+e^-)$ [eV]	0.43	0.046	0.367	0.1
$\Gamma(\chi_{c_2} \to e^+e^-)$ [eV]	4.25	0.037	0.137	–

$$
\begin{aligned}
A(p_1,p_2) &= \frac{2}{\sqrt{6}M_{\chi c0}}\Big[(\epsilon^1\epsilon^2)(p_1p_2) - (\epsilon^1 p_2)(\epsilon^2 p_1)\Big] \\
&\quad \times \Big[M^2_{\chi c0} + (p_1p_2)\Big], \\
c^0_\gamma &= \frac{16\pi\alpha}{\sqrt{m}} \cdot (a + \frac{f\cdot a_J^0}{M^2_{J/\psi}} + \frac{f'\cdot a^0_{\psi'}}{M^2_{\psi'}}) \cdot \frac{1}{(M^2_{\chi c0}/4 + m^2)^2}, \\
c^0_{J/\psi} &= \frac{4\cdot e\cdot a_J^0}{\sqrt{m}} \cdot \frac{1}{(M^2_{\chi c0}/4 + m^2 - M^2_{J/\psi}/2)^2}, \\
c^0_{\psi'} &= \frac{4\cdot e\cdot a^0_{\psi'}}{\sqrt{m}} \cdot \frac{1}{(M^2_{\chi c0}/4 + m^2 - M^2_{\psi'}/2)^2},
\end{aligned}
\tag{2}
$$

with $f = \sqrt{\frac{3\Gamma_{J/\psi\to e^+e^-}M^3_{J/\psi}}{4\pi\alpha^2}}$ and $f' = \sqrt{\frac{3\Gamma_{\psi'\to e^+e^-}M^3_{\psi'}}{4\pi\alpha^2}}$. Most of the couplings are defined in [1]: a is proportional to the derivative of the wave function at the origin, m is the effective charm quark mass, a_J and $a_{\psi'}$ are the couplings of $J/\psi - \chi_{c_i} - \gamma$ and $\psi' - \chi_{c_i} - \gamma$ ($i = 1,2$; not appearing in Eq. (2)). a_J^0 and $a^0_{\psi'}$ denote the couplings of $J/\psi - \chi_{c_0} - \gamma$ and $\psi' - \chi_{c_0} - \gamma$ respectively.

The coupling constants can be extracted from the experimental data adding to the ones used in [1] the following widths

$$
\begin{aligned}
\Gamma(\chi_{c0} \to \gamma\gamma) &= \frac{3}{128\pi}|c^0_\gamma|^2 M^5_{\chi c0}, \\
\Gamma(\chi_{c0} \to J/\psi\gamma) &= \frac{1}{192\pi}|c^0_{J/\psi}|^2 M^5_{\chi c0}(3-x)^2(1-x)^3, \\
\Gamma(\psi' \to \chi_{c0}\gamma) &= \frac{1}{576\pi}|c^0_{\psi'}|^2(1-y)^3(1-3y)^2\frac{M^5_{\psi'}}{y},
\end{aligned}
\tag{3}
$$

where $x = M^2_{J/\psi}/M^2_{\chi_{c_0}}$ and $y = M^2_{\chi_{c_0}}/M^2_{\psi'}$.

The fit to 8 experimental values ($\Gamma(\chi_{c_0} \to \gamma\gamma)$, $\Gamma(\chi_{c_2} \to \gamma\gamma)$, $\Gamma(\chi_{c_i} \to J/\psi\gamma)$, $i = 0,1,2$, $\Gamma(\psi' \to \chi_{c_i}\gamma)$, $i = 0,1,2$) with 6 model parameters (a, m, a_J, a_J^0, $a_{\psi'}$ and $a^0_{\psi'}$) gives $\chi^2 = 0.94$. The Eqs. (26)–(30) from [1] and Eqs. (3) from this letter were used as model predictions. The fit results are summarised in Table 1.

The model parameters describing χ_{c1} and χ_{c2} are very close to the model parameters obtained in [1] and the predictions for the electronic widths ($\Gamma(\chi_{c_1} \to e^+e^-) = 0.37$ eV and $\Gamma(\chi_{c_2} \to e^+e^-) = 3.86$ eV) did change within the parametric uncertainty of the model, which is about 10%. The $a^0_{\psi'}$ coupling is positive at difference with the negative $a_{\psi'}$. Both signs are the only ones allowed by the fit.

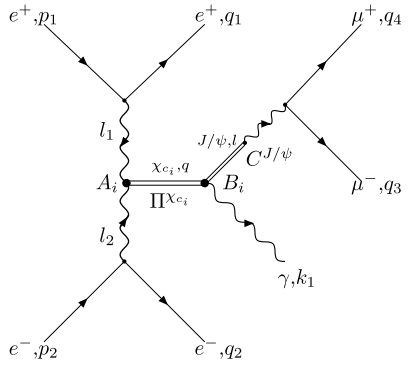

Fig. 1. The Feynman diagram for the amplitude of the reaction $e^+e^- \to e^+e^-\chi_{c_i}(\to J/\psi(\to \mu^+\mu^-)\gamma)$. The notation of four momenta is used in the formulae presented in this letter.

The χ_{c1} and χ_{c2} electronic widths are calculated as loop integrals (see Fig. 5 of [1]), thus the $\chi_{ci} - \gamma^* - \gamma^*$, $\chi_{ci} - J/\psi^* - \gamma^*$ and $\chi_{ci} - \psi'^* - \gamma^*$ form factors are crucial for the theoretical predictions. Table 2 summarises the situation. All the models referenced there give correct predictions for the $\chi_{c_i} \to J/\psi\gamma$, $i = 1,2$ and $\chi_{c_2} \to \gamma\gamma$ partial decay widths. Yet, the predictions for the χ_{c1} and χ_{c2} electronic widths are different up to two orders of magnitude, showing why the experimental studies of the $\chi_{ci} - \gamma^* - \gamma^*$, $\chi_{ci} - J/\psi^* - \gamma^*$ and $\chi_{ci} - \psi'^* - \gamma^*$ form factors are important. The ψ' contribution is taken into account only in [6] and [1]. The contributions taken into account in [6] and [1] are qualitatively the same, yet the differences coming from loop integrals are striking and require further studies.

3. The amplitudes and the cross section

With the couplings obtained from the fit one can predict the rates for the reactions $e^+e^- \to e^+e^-\chi_{c_i}$ and $e^+e^- \to e^+e^-\chi_{c_i}(\to J/\psi(\to \mu^+\mu^-)\gamma)$. We do consider here only signal processes with the Feynman diagram given in Fig. 1. The QED non-resonant background can be suppressed by requiring that the $\mu^+\mu^-\gamma$ invariant mass is close to the χ_{ci} mass and the $\mu^+\mu^-$ invariant mass is close to the J/ψ mass. Its size is estimated in Section 4. As the χ_{ci} and J/ψ are almost on-shell we use a constant $\chi_{ci} - J/\psi - \gamma$ form factor.

The relevant amplitudes, with the four momenta denoted in Fig. 1, read

$$
\begin{aligned}
M_0 &= e^3 V_\nu(p_1,q_1)\, A_0^{\nu\mu}(l_1,l_2)\; U_\mu(p_2,q_2) W^\beta(q_3,q_4)\\
&\quad\times \Pi^{\chi_{c0}}(q)\; B_0^\sigma(l,k_1)\; C_{\sigma\beta}^{J/\Psi}(l^2)\\
M_1 &= e^3 V_\nu(p_1,q_1)\, A_1^{\nu\mu\omega}(l_1,l_2)\; U_\mu(p_2,q_2) W^\beta(q_3,q_4)\\
&\quad\times \Pi^{\chi_{c1}}_{\omega\delta}(q)\; B_1^{\delta\sigma}(l,k_1)\; C_{\sigma\beta}^{J/\Psi}(l^2)\\
M_2 &= e^3 V_\nu(p_1,q_1)\, A_2^{\nu\mu\omega\delta}(l_1,l_2) U_\mu(p_2,q_2) W^\beta(q_3,q_4)\\
&\quad\times \Pi^{\chi_{c2}}_{\omega\delta\pi\xi}(q) B_2^{\pi\xi\sigma}(l,k_1) C_{\sigma\beta}^{J/\Psi}(l^2)
\end{aligned}
\tag{4}
$$

with

$$
\begin{aligned}
A_0^{\nu\mu}(l_1,l_2) &= \frac{2\tilde{c}_\gamma^0((l_1-l_2)^2)}{\sqrt{6}M_{\chi_{c0}}}\\
&\quad\times\left[\left(g^{\nu\mu}(l_1\cdot l_2)-l_1^\mu l_2^\nu\right)(M_{\chi_{c0}}^2+l_1\cdot l_2)-g^{\nu\mu}l_1^2l_2^2\right],\\
B_0^\sigma(l,k_1) &= \frac{2c_{J/\psi}^0}{\sqrt{6}M_{\chi_{c0}}}F^{1\sigma\nu}(k_1)l_\nu(M_{\chi_{c0}}^2+k_1\cdot l),\\
A_1^{\nu\mu\omega}(l_1,l_2) &= -i\tilde{c}_\gamma^1((l_1-l_2)^2)\left(\epsilon^{\bar\nu\nu\mu\omega}\left(l_{2\bar\nu}l_1^2-l_{1\bar\nu}l_2^2\right)\right.\\
&\quad\left.+\epsilon^{\bar\mu\bar\nu\mu\omega}l_{1\bar\mu}l_{2\bar\nu}l_1^\nu-\epsilon^{\bar\nu\bar\mu\nu\omega}l_{1\bar\nu}l_{2\bar\mu}l_2^\mu\right),\\
B_1^{\delta\sigma}(l,k_1) &= -\frac{i}{2}c_{J/\psi}^1\left(\epsilon^{\bar\mu\bar\nu\sigma\delta}F^1_{\bar\mu\bar\nu}(k_1)l^2-\epsilon^{\bar\mu\bar\nu\bar\alpha\delta}F^1_{\bar\mu\bar\nu}(k_1)l_{\bar\alpha}l^\sigma\right),\\
A_2^{\nu\mu\omega\delta}(l_1,l_2) &= -\tilde{c}_\gamma^2((l_1-l_2)^2)\sqrt{2}M_{\chi_{c2}}\left(g^{\mu\delta}l_1^\omega l_2^\nu-g^{\nu\mu}l_1^\omega l_2^\delta\right.\\
&\quad\left.-g^{\nu\omega}g^{\mu\delta}(l_1\cdot l_2)+g^{\nu\omega}l_1^\mu l_2^\delta\right),\\
B_2^{\pi\xi\sigma}(l,k_1) &= -c_{J/\psi}^2\sqrt{2}M_{\chi_{c2}}\left(F^{1\bar\beta\pi}(k_1)g^{\sigma\xi}l_{\bar\beta}-F^{1\sigma\pi}(k_1)l^\xi\right),\\
\tilde{c}_\gamma^0((l_1-l_2)^2) &= \frac{16\pi\alpha}{\sqrt{m}}\left(a+\frac{fa_J^0}{M_{J/\psi}^2}+\frac{f'a_{\psi'}^0}{M_{\psi'}^2}\right)\\
&\quad\times\frac{1}{((l_1-l_2)^2/4-m^2+i\epsilon)^2},\\
\tilde{c}_\gamma^i((l_1-l_2)^2) &= \frac{16\pi\alpha}{\sqrt{m}}\left(a+\frac{fa_J}{M_{J/\psi}^2}+\frac{f'a_{\psi'}}{M_{\psi'}^2}\right)\\
&\quad\times\frac{1}{((l_1-l_2)^2/4-m^2+i\epsilon)^2},\ i=1,2,\\
c_{J/\psi}^i &= \frac{4\cdot e\cdot a_J}{\sqrt{m}}\cdot\frac{1}{(M_{\chi_{c_i}}^2/4+m^2-M_{J/\psi}^2/2)^2},\ i=1,2,\\
C_{\sigma\beta}^{J/\psi}(l^2) &= \sqrt{\frac{3\Gamma_{J/\psi\to e^+e^-}}{\alpha\sqrt{l^2}}}\frac{g_{\sigma\beta}}{l^2-M_{J/\psi}^2+i\Gamma_{J/\psi}M_{J/\psi}},\\
F^1_{\mu\nu}(k_1) &= (\epsilon_\mu^1 k_{1\nu}-\epsilon_\nu^1 k_{1\mu}),\\
\Pi^{\chi_{c0}}(q) &= \frac{1}{q^2-M_{\chi_{c0}}^2+i\Gamma_{\chi_{c0}}M_{\chi_{c0}}},\\
\Pi^{\chi_{c1}}_{\omega\delta}(q) &= \frac{g_{\omega\delta}-q_\omega q_\delta/M_{\chi_{c1}}^2}{q^2-M_{\chi_{c1}}^2+i\Gamma_{\chi_{c1}}M_{\chi_{c1}}},\\
\Pi^{\chi_{c2}}_{\omega\delta\pi\xi}(q) &= \frac{\frac{1}{2}(P_{\omega\pi}P_{\delta\xi}+P_{\omega\xi}P_{\delta\pi})-\frac{1}{3}(P_{\omega\delta}P_{\pi\xi})}{q^2-M_{\chi_{c2}}^2+i\Gamma_{\chi_{c2}}M_{\chi_{c2}}},\\
P_{\mu\nu} &= -g_{\mu\nu}+q_\mu q_\nu/M_{\chi_{c2}}^2,\qquad V_\nu(p_1,q_1)=\frac{\overline{v}(p_1)\gamma_\nu v(q_1)}{(q_1-p_1)^2},\\
U_\mu(p_2,q_2) &= \frac{\overline{u}(q_2)\gamma_\mu u(p_2)}{(q_2-p_2)^2},\qquad W^\beta(q_3,q_4)=\overline{u}(q_3)\gamma^\beta v(q_4)
\end{aligned}
\tag{5}
$$

where ϵ_μ^1 is the photon polarisation vector. The parts of the $\chi_{c_i}-\gamma^*-\gamma^*$ vertex vanishing when contracted with the $e-e-\gamma^*$ vertices are not shown in the above formulae. The A_i, $i=0,1,2$ tensors denote the $\gamma^*-\gamma^*-\chi_{c_i}^*$ vertices, while the B_i, $i=0,1,2$ tensors stand for $\gamma^*-J/\psi^*-\chi_{c_i}^*$ vertices. Generally more tensors structures are allowed [3], thus the results obtained in this letter are specific to the adopted model. The amplitudes were implemented into the event generator EKHARA [9,8]. Two independent codes were built using two different methods of spin summations to cross check the implementation.

In principle the amplitudes should be added coherently as the final state is the same for all $\chi_{c_i}^*$ intermediate states. However all the amplitudes drop rapidly, when the invariant mass is a bit off-resonance. At about 4 decay widths off-resonance the cross sections drop to 1% of the peak values. As a result the interferences can be safely neglected. Yet, the detector resolution effects, typically of order of 10–20 MeV, can result in 'moving' the events between different χ_{c_i} samples. An option of simulating simultaneously of all χ_{c_i} production is available in the EKHARA generator to facilitate this simulation. The interferences between amplitudes are not taken into account to speed up the calculations.

For the phase space generation of the $e^+e^-\to e^+e^-\chi_{c_i}$ reaction the method used in [9] for the generation of the phase space for reactions $e^+e^-\to e^+e^-P$ ($P=\pi^0,\eta,\eta'$) was adopted. For the simulation of the reaction $e^+e^-\to e^+e^-\chi_{c_i}$ ($\to J/\psi(\to\mu^+\mu^-)\gamma$) the phase space generation is split into two parts: the first part generates the e^+,e^- and the virtual χ_{c_i} four momenta, while the second part generates the μ^+,μ^- and γ four momenta. In the first part the virtual χ_{c_i} invariant mass was generated using the standard change of variables to absorb the Breit–Wigner peak coming from χ_{c_i} propagator, while the remaining variables were generated using the same method as in $e^+e^-\to e^+e^-\chi_{c_i}$ reaction. In the second part the invariant mass l^2 was generated using the standard change of variables to absorb the Breit–Wigner peak coming from J/ψ propagator, the photon angles were generated flat in the rest frame of the virtual χ_{c_i}, while the $\mu^+(\mu^-)$ angles were generated flat in the virtual J/ψ rest frame. In the mode, where all 3 χ_{c_i} are generated simultaneously the 3-channel Monte Carlo variance reduction was used. The phase space generation was cross checked with an independent computer code, which uses the representation described in [10], with flat generation of all variables.

The χ_{c_i} production cross section in the reaction $e^+e^-\to e^+e^-\chi_{c_i}$ (the amplitudes are easy to infer from Eq. (4)) integrated over the complete phase space with the integrated luminosity of BELLE II of 50 ab^{-1} leads to the expected number of events of about 140M (χ_{c_0}), 4.3M (χ_{c_1}) and 142M (χ_{c_2}). These rates will allow for detailed studies of many χ_{c_i} decay modes. Unfortunately the measurement of electronic width of χ_{c_1} through measurement of the cross section of the reaction $e^+e^-\to e^+e^-\chi_{c_1}(\to e^+e^-)$ is out of reach as the predicted number of events is about 2. For χ_{c_2} the situation is a bit better with an expected number of events equal to 284. Further drop is however expected as the detector does not cover the complete solid angle range.

If one tags a positron, in the reaction $e^+e^-\to e^+e^-\chi_{c_i}$, in the angular range between 17° and 150° assuming asymmetric beams of 4 and 7 GeV with half crossing angles of 41.5 mrad, the expected number of events drops to 6.7M (χ_{c_0}), 1.4M (χ_{c_1}) and 7.2M (χ_{c_2}). It shows that one has an access to information about $\chi_{c_i}-\gamma^*-\gamma$ form factors. The event distribution as a function virtual photon invariant mass ($l_1^2=(p_1-q_1)^2$) is shown in Fig. 2. When both electron and positron are observed in the given above angular range the expected number of events in the reactions $e^+e^-\to e^+e^-\chi_{c_i}$ are equal to 249k (χ_{c_0}), 174k (χ_{c_1}) and 295k (χ_{c_2}). It promises decent statistics in measurements with doubly tagged events.

In this letter we concentrate on the possible tests of the models of $\chi_{c_i} - \gamma^* - \gamma^*$ form factors using single and double tag events relying on an identification of a simple χ_{c_i} decay mode: $\chi_{c_i} \to J/\psi(\to \mu^+\mu^-)\gamma$. If one requires identification of χ_{c_i} and J/ψ through invariant masses of $\mu^+\mu^-\gamma$ and $\mu^+\mu^-$ final states respectively, the $\chi_{c_i} - J/\psi^* - \gamma$ form factors are entering the cross section with fixed invariants, thus they are almost constant. This way the $\chi_{c_i} - \gamma^* - \gamma$ form factors can be measured.

In the results presented below we assume the asymmetric beams of 4 and 7 GeV with half crossing angles of 41.5 mrad. We assume also that the particles (μ^+, μ^-, photon and positron and/or electron) can be detected and their four momenta measured if their polar angles are between 17° and 150° [11].

If the electron is not tagged, the expected numbers of events after the applied cuts are 3114 for χ_{c_0}, 21819 for χ_{c_1} and 44126 for χ_{c_2}. It will allow for testing of the $\chi_{c_i} - \gamma^* - \gamma$ form factors for the first time. The l_1^2 invariant mass distribution is shown in Fig. 3. The l_2^2 invariant mass is, as expected, limited to small values with 2770 (χ_{c_0}), 17892 (χ_{c_1}) and 38863 (χ_{c_2}) events with $-1\ \text{GeV}^2 < l_2^2 < 0$. Thus the form factor can be extracted with a decent accuracy for one of the invariants close to zero and the second spanning up to about $-30\ \text{GeV}^2$. With a limited statistics one can even have data for χ_{c_1} (2538 events) and χ_{c_2} (2472 events) with all the particles observed in the detector allowing for an accurate reconstruction of both invariants. The expected event distributions are shown in Fig. 4. For χ_{c_0} the expectation is 136 events.

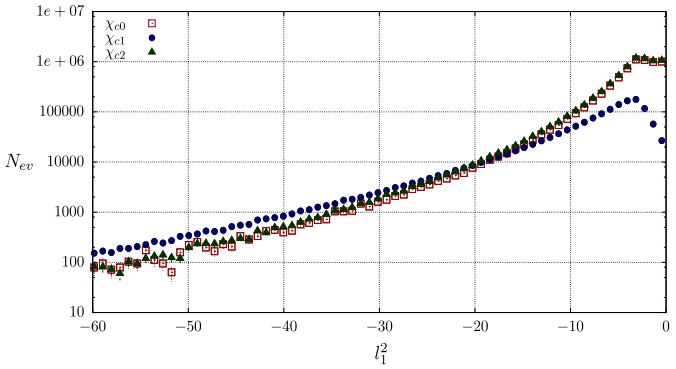

Fig. 2. The distributions of expected number of events (N_{ev}) for χ_{c_i} production, when one observes the positron in the angular range of 17° and 150°.

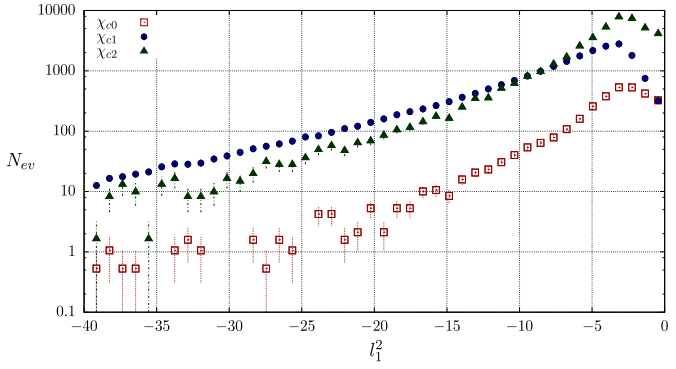

Fig. 3. The distributions of expected number of events (N_{ev}) for χ_{c_i} production with subsequent decay to $J/\psi(\to \mu^+\mu^-) - \gamma$. The event selection is described in the text.

4. QED background estimates

The non-resonant QED background estimation was performed using the HELAC-PHEGAS generator [12]. The event selections were identical to the ones used to obtain the signal events. The ranges of $\mu^+\mu^-$ and $\mu^+\mu^-\gamma$ invariant masses were chosen to contain 99% of the signal cross section: $3.0965 \le l^2 \le 3.0973$, $3.37 \le q^2 \le 3.50$ for χ_{c0}, $3.50191 \le q^2 \le 3.51941$ for χ_{c1}, $3.5475 \le q^2 \le 3.5650$ for χ_{c2}. The polar angles of the observed particles ($\mu^+\mu^-\gamma e^+$ for single tag events and $\mu^+\mu^-\gamma e^+e^-$ for double tag events) were required to be between 17° and 150° in the laboratory frame (see Section 3). For χ_{c_0} production and decay the background is not negligible: 110% for single tag events and 220% for double tag events. It shows that in this case the interference effects between background and signal are important and will have to be studied. Yet, as the signal is small as compared to χ_{c_1} and χ_{c_2} the expected statistical accuracy will also be much worse. For χ_{c_1} and χ_{c_2} the background to signal ratio is much smaller for two reasons: the signals are bigger by one order of magnitude and the decay widths are smaller about one order of magnitude as compared to χ_{c_0} decay width. For single tag events the background to signal ratio is 0.2% for χ_{c_1} and 0.7% for χ_{c_2}, while for double tag events it is 0.1% and 1.7% respectively. Thus for χ_{c_1} and χ_{c_2} the interferences between background and signal amplitudes can be neglected and the background can be simulated using the existing Monte Carlo generators. The resonant background, mainly the $e^+e^- \to e^+e^- J/\psi(\to \mu^+\mu^-)\gamma$ process without χ_{c_i} intermediate states involved, should also be studied. None of the existing generators is currently able to generate this process and the main difficulty will be to find an efficient generation algorithm.

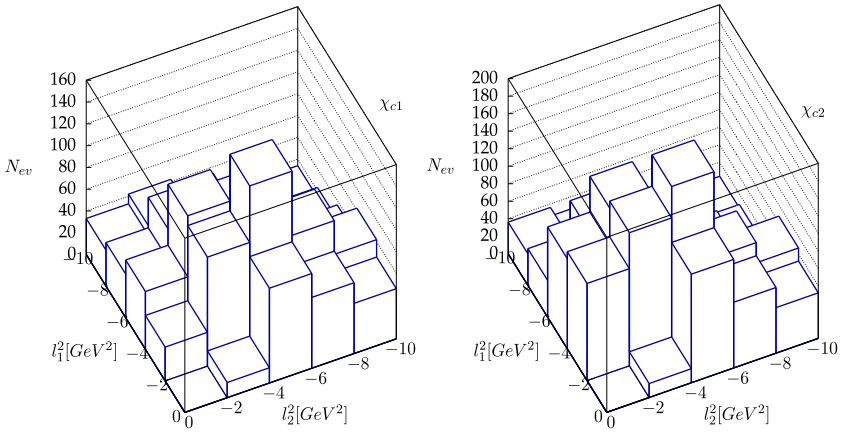

Fig. 4. The distributions of expected number of events (N_{ev}) for χ_{c_1} and for χ_{c_2} production with subsequent decay to $J/\psi(\to \mu^+\mu^-) - \gamma$ when both electron and positron are tagged. The event selection is described in the text.

5. Conclusions

The model of the $\chi_{c_i} - \gamma^* - \gamma^*$, $\chi_{c_i} - J/\psi^* - \gamma^*$ form factors developed in [1] for χ_{c_1} and χ_{c_2} is extended to χ_{c_0} case. Within this model, it was shown that at BELLE II it will be possible to study in detail $\chi_{c_i} - \gamma^* - \gamma^*$ form factors through measurements of the reaction $e^+e^- \to e^+e^-\chi_{c_i}(\to J/\psi(\to \mu^+\mu^-)\gamma)$. It is achieved by event selections, which force the χ_{ci} and J/ψ to be almost on-shell. For these kinematic configurations the interference between the signal and the QED background is negligible for χ_{c1} and χ_{c2}, while for χ_{c0} it has to be taken into account. The proposed measurements should clarify, which of the models giving predictions for the χ_{c_1} and χ_{c_2} electronic widths is correct, even without direct measurement of these widths. If the electronic widths are measured as well, they will allow for further refinements of the models. The expected number of events for the χ_{c_i} production show that detailed studies of the χ_{c_i} branching ratios will also be possible at BELLE II. The newly updated Monte Carlo generator EKHARA can be of help for the visibility studies and the data analyses.

References

[1] H. Czyz, J.H. Kühn, S. Tracz, χ_{c1} and χ_{c2} production at e^+e^- colliders, Phys. Rev. D 94 (3) (2016) 034033, http://dx.doi.org/10.1103/PhysRevD.94.034033, arXiv:1605.06803.

[2] T. Aushev, et al., Physics at Super B Factory, arXiv:1002.5012.

[3] J.H. Kühn, J. Kaplan, E.G.O. Safiani, Electromagnetic annihilation of e^+e^- into quarkonium states with even charge conjugation, Nucl. Phys. B 157 (1979) 125, http://dx.doi.org/10.1016/0550-3213(79)90055-5.

[4] D. Yang, S. Zhao, $\chi_{Q\,J} \to l^+l^-$ within and beyond the Standard Model, Eur. Phys. J. C 72 (2012) 1996, http://dx.doi.org/10.1140/epjc/s10052-012-1996-z, arXiv:1203.3389.

[5] A. Denig, F.-K. Guo, C. Hanhart, A.V. Nefediev, Direct X(3872) production in e^+e^- collisions, Phys. Lett. B 736 (2014) 221–225, http://dx.doi.org/10.1016/j.physletb.2014.07.027, arXiv:1405.3404.

[6] N. Kivel, M. Vanderhaeghen, $\chi_{c\,J} \to e^+e^-$ decays revisited, J. High Energy Phys. 02 (2016) 032, http://dx.doi.org/10.1007/JHEP02(2016)032, arXiv:1509.07375.

[7] C. Patrignani, et al., Review of particle physics, Chin. Phys. C 40 (10) (2016) 100001, http://dx.doi.org/10.1088/1674-1137/40/10/100001.

[8] H. Czyz, E. Nowak-Kubat, The reaction $e^+e^- \to e^+e^-\pi^+\pi^-$ and the pion form-factor measurements via the radiative return method, Phys. Lett. B 634 (2006) 493–497, http://dx.doi.org/10.1016/j.physletb.2006.02.024, arXiv:hep-ph/0601169.

[9] H. Czyz, S. Ivashyn, EKHARA: a Monte Carlo generator for $e^+e^- \to e^+e^-\pi^0$ and $e^+e^- \to e^+e^-\pi^+\pi^-$ processes, Comput. Phys. Commun. 182 (2011) 1338–1349, http://dx.doi.org/10.1016/j.cpc.2011.01.029, arXiv:1009.1881.

[10] H. Czyz, J.H. Kuhn, Four pion final states with tagged photons at electron positron colliders, Eur. Phys. J. C 18 (2001) 497–509, http://dx.doi.org/10.1007/s100520000553, arXiv:hep-ph/0008262.

[11] T. Abe, et al., Belle II Technical Design Report, arXiv:1011.0352.

[12] A. Cafarella, C.G. Papadopoulos, M. Worek, Helac-Phegas: a generator for all parton level processes, Comput. Phys. Commun. 180 (2009) 1941–1955, http://dx.doi.org/10.1016/j.cpc.2009.04.023, arXiv:0710.2427.